JCTC Journal of Chemical Theory and Computation

Article

pubs.acs.org/JCTC

The R^{-7} Dispersion Interaction in the General Effective Fragment Potential Method

Peng Xu, Federico Zahariev, and Mark S. Gordon*

Department of Chemistry, Iowa State University, Ames, Iowa 50011, United States

Supporting Information

ABSTRACT: The R^{-7} term (E7) in the dispersion expansion is developed in the framework of the general effective fragment potential (EFP2) method, formulated with the dynamic anisotropic Cartesian polarizability tensors over the imaginary frequency range. The E7 formulation is presented in terms of both the total molecular polarizability and the localized molecular orbital (LMO) contributions. An origin transformation from the center of mass to the LMO centroids is incorporated for the computation of the LMO dipole−quadrupole polarizability. The two forms considered for the damping function for the R^{-7} dispersion interaction, the overlap-based and Tang−Toennies damping functions, are extensions of the existing damping functions for the R^{-6} term in the dispersion expansion. The R^{-7} dispersion interaction is highly orientation dependent: it can be either attractive or repulsive, and its magnitude can change substantially as the relative orientation of two interacting molecules changes. Although the R^{-7} dispersion energy rotationally averages to zero, it may be significant for systems in which rotational averaging does not occur, such as rotationally rigid molecular systems as in molecular solids or constrained surface reactions.

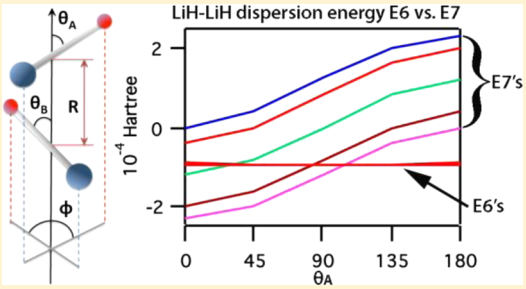

I. INTRODUCTION

The dispersion interaction, a nonclassical phenomenon, arises from the correlated movement of electrons. In the language of a multipole description of the charge distributions of molecules, it can be thought of as the interaction between induced multipoles. Although weak, the dispersion interaction plays an important role in many phenomena. For example, the dispersion contribution to the water−water hydrogen bond is nontrivial,[1] dispersion is a key component in π-stacking interactions[2−5] and provides the essence of the binding of noble gases.[6,7]

The dispersion interaction energy is often expressed as an expansion in inverse powers of the interatomic or intermolecular distance:[8]

$$E_{\mathrm{disp}} = C_6R^{-6} + C_7R^{-7} + C_8R^{-8} + \ldots \quad (1)$$

The C_n coefficients in eq 1 are expansion coefficients that may be derived from first principles or fitted in some manner, and each term corresponds to one or more induced multipole-induced multipole interactions. The dispersion interaction can be formulated in terms of second-order Rayleigh−Schrödinger perturbation theory, where the perturbation operator is expressed as multipole expansions of the two interacting molecules.[9] The R^{-6} dispersion interaction term is accounted for by using the dynamic dipole−dipole polarizability over the imaginary frequency range.[10] The R^{-7} dispersion term arises from the mixing of dipole−dipole interactions with dipole−quadrupole interactions.[11] In this paper the R^{-7} contribution to the dispersion energy will be called E7 for brevity. E7 is zero for atoms and centrosymmetric molecules. For noncentrosymmetric molecules, E7 does depend on the relative orientation of the molecules,[9,11] and that is an important consideration.

The effective fragment potential (EFP) method, developed by Gordon and co-workers,[12] is a discrete method for studying the entire range of intermolecular interactions. The original implementation, EFP1, was designed solely for water and involves a fitted repulsive potential. The second implementation, the general effective fragment potential (EFP2) method contains no fitted parameters and can be generated for any (closed-shell) molecule. In this paper, EFP2 will be called EFP unless a distinction between EFP1 and EFP2 needs to be made. The interaction energy between two molecules/fragments is calculated using properties of the two isolated molecules. The required properties are generated in a prior MAKEFP calculation. The interaction energy is divided into five components, which may be classified in two categories: the Coulomb interaction, polarization/induction, and dispersion are long-range interactions ($U \sim R^{-n}$). Exchange repulsion and charge transfer are short-range interactions ($U \sim e^{-\alpha R}$).

The EFP Coulomb interaction is modeled by the Stone distributed multipolar analysis (DMA) method.[13,14] The multipole expansion is truncated at the octopole term, and the expansion centers are the nuclei and bond midpoints.[12] The EFP polarization term arises from the interaction between an induced dipole on one fragment and the electric field due to all of the other fragments.[12] It is modeled with localized molecular orbital (LMO) anisotropic static dipole polarizability tensors.

Received: January 9, 2014
Published: February 7, 2014

   dx.doi.org/10.1021/ct500017n | J. Chem. Theory Comput. 2014, 10, 1576−1587

The induced dipole is iterated to self-consistency, thereby introducing many-body effects. The exchange repulsion term is obtained from a power expansion of the intermolecular LMO overlap integral, truncated at the second order in the current implementation.[15] Charge transfer (CT) is the interaction between the occupied orbitals of one molecule and the virtual orbitals of another molecule. The CT interaction between two EFP fragments is derived from a second-order perturbative approach.[16,17] A power expansion of the intermolecular overlap is used for the CT term as well, but the truncation is at first order. The leading term in the dispersion interaction, which will be discussed in Section II, is described using the dynamic (frequency-dependent) isotropic dipole polarizability of LMOs over the imaginary frequency range.[18] This gives rise to the isotropic R^{-6} dispersion energy. Currently, the higher order dispersion energy is approximated as one-third of this isotropic R^{-6} energy. The goal of this paper is to derive an explicit expression for E7 and to evaluate the relative importance of this term.

This paper is organized as follows: Section II presents a detailed derivation of E7, in terms of the Cartesian molecular dynamic polarizability tensors and in terms of LMO dynamic polarizability tensors. Implementation of the polarizability and damping functions is also described. Computational details, including the benchmarking system LiH···LiH and other dimer systems, are described in Section III. Results are presented and discussed in Section IV. Conclusions and future work are provided in Section V.

II. THEORY

In the framework of Rayleigh−Schrödinger perturbation theory (RSPT), the dispersion interaction energy between two closed-shell nondegenerate ground-state molecules is part of the second-order interaction energy:[9,19]

$$E^{\mathrm{disp}} = -\sum_{\substack{m\neq 0\\ n\neq 0}} \frac{\langle 0_A 0_B|\hat{V}|mn\rangle\langle mn|\hat{V}|0_A 0_B\rangle}{E_m^A + E_n^B - E_0^A - E_0^B} \tag{2}$$

where 0_A and 0_B are the ground states of molecules A and B, respectively, and m and n are the excited states of molecules A and B, respectively. Correspondingly, E_m^A is the energy of the m^{th} excited state of molecule A. The other Es are similarly defined. The unperturbed Hamiltonian is the sum of the Hamiltonians of the isolated molecules A and B.

$$\hat{H}_0 = \hat{H}_0^A + \hat{H}_0^B \tag{3}$$

The perturbation operator $\hat{V}$ is the interaction operator, which contains the electrostatic interaction between the constituent particles. By expressing the charge distributions of the two molecules A and B as two multipole expansions, one can express the interaction operator as

$$\hat{V} = \mathbf{T}^{AB} q^A q^B + \sum_{\alpha}^{x,y,z} \mathbf{T}_{\alpha}^{AB}(q^A \mu_{\alpha}^B - \mu_{\alpha}^A q^B) - \sum_{\alpha,\beta}^{x,y,z} \mathbf{T}_{\alpha\beta}^{AB} \mu_{\alpha}^A \mu_{\beta}^B - \frac{1}{3}\sum_{\alpha\beta\gamma}^{x,y,z} \mathbf{T}_{\alpha\beta\gamma}^{AB}(\mu_{\alpha}^A \theta_{\beta\gamma}^B - \theta_{\alpha\beta}^A \mu_{\gamma}^B)... \tag{4}$$

where q^A is the total charge on molecule A, μ_{α}^B is the αth component of the dipole moment of molecule B. $\theta_{\beta\gamma}^B$ is the $\beta\gamma$th component of the quadrupole moment of B. The electrostatic $\mathbf{T}$ tensors are defined as follows:

$$\mathbf{T}^{AB} = \frac{1}{4\pi\varepsilon_0 R} \tag{5a}$$

$$\mathbf{T}_{\alpha}^{AB} = \frac{1}{4\pi\varepsilon_0}\nabla_{\alpha}\frac{1}{R} = -\frac{R_{\alpha}}{4\pi\varepsilon_0 R^3} \tag{5b}$$

$$\mathbf{T}_{\alpha\beta}^{AB} = \frac{1}{4\pi\varepsilon_0}\nabla_{\alpha}\nabla_{\beta}\frac{1}{R} = \frac{3R_{\alpha}R_{\beta} - R^2\delta_{\alpha\beta}}{4\pi\varepsilon_0 R^5} \tag{5c}$$

$$\mathbf{T}_{\alpha\beta\gamma}^{AB} = \frac{1}{4\pi\varepsilon_0}\nabla_{\alpha}\nabla_{\beta}\nabla_{\gamma}\frac{1}{R} = -\frac{15R_{\alpha}R_{\beta}R_{\gamma} - 3R^2(R_{\alpha}\delta_{\beta\gamma} + R_{\beta}\delta_{\alpha\gamma} + R_{\gamma}\delta_{\alpha\beta})}{4\pi\varepsilon_0 R^7} \tag{5d}$$

where $\mathbf{R} = \mathbf{B} - \mathbf{A}$. Here $\mathbf{B}$ and $\mathbf{A}$ are the expansion center coordinates at which the multipole expansions are obtained. At this stage, only a single-center multipole expansion for each molecule is carried out. There is some arbitrariness in the definition of the multipoles because the choice of the expansion center is arbitrary. The charge is a scalar and is independent of the expansion center. The dipole moment of a neutral molecule is invariant under a change of the expansion center.[9] However, the higher moments, such as quadrupole moments, depend on the location of the expansion center. In the literature, this phenomenon is commonly referred to as "origin dependence";[9,11] in this work the word "origin" refers to the expansion center. The convention that is used here is discussed in subsequent sections.

Consider the total wave function of a system AB in the long-range approximation, where there is no significant overlap between the two molecular wave functions and hence no exchange effect, then the total wave function is the Hartree product of the individual wave functions:

$$|0_A 0_B\rangle = |0_A\rangle|0_B\rangle \text{ and } |mn\rangle = |m\rangle|n\rangle \tag{6}$$

Truncating the interaction operator (eq 4) at the dipole−quadrupole term and substituting eqs 4 and 6 into eq 2 gives

$$\begin{aligned} E^{\mathrm{disp}} = -\sum_{\substack{m\neq 0\\ n\neq 0}} \Bigg\{ & \langle 0_A|\langle 0_B|\sum_{\alpha\beta}^{x,y,z} \mathbf{T}_{\alpha\beta}^{AB}\mu_{\alpha}^A\mu_{\beta}^B|m\rangle|n\rangle\langle m|\langle n|\sum_{\gamma\sigma}^{x,y,z} \mathbf{T}_{\gamma\sigma}^{AB}\mu_{\gamma}^A\mu_{\sigma}^B|0_A\rangle|0_B\rangle \\ & + \langle 0_A|\langle 0_B|\sum_{\alpha\beta}^{x,y,z} \mathbf{T}_{\alpha\beta}^{AB}\mu_{\alpha}^A\mu_{\beta}^B|m\rangle|n\rangle\langle m|\langle n|\left(\frac{1}{3}\sum_{\gamma\sigma\kappa}^{x,y,z} \mathbf{T}_{\gamma\sigma\kappa}^{AB}(\mu_{\gamma}^A\theta_{\sigma\kappa}^B - \theta_{\gamma\sigma}^A\mu_{\kappa}^B)\right) \\ & \times |0_A\rangle|0_B\rangle + \langle 0_A|\langle 0_B|\left(\frac{1}{3}\sum_{\alpha\beta\gamma}^{x,y,z} \mathbf{T}_{\alpha\beta\gamma}^{AB}(\mu_{\alpha}^A\theta_{\beta\gamma}^B - \theta_{\alpha\beta}^A\mu_{\gamma}^B)\right) \\ & \times |m\rangle|n\rangle\langle m|\langle n|\sum_{\sigma\kappa}^{x,y,z} \mathbf{T}_{\sigma\kappa}^{AB}\mu_{\sigma}^A\mu_{\kappa}^B|0_A\rangle|0_B\rangle + \langle 0_A|\langle 0_B| \\ & \times \left(\frac{1}{3}\sum_{\alpha\beta\gamma}^{x,y,z} \mathbf{T}_{\alpha\beta\gamma}^{AB}(\mu_{\alpha}^A\theta_{\beta\gamma}^B - \theta_{\alpha\beta}^A\mu_{\gamma}^B)\right) \\ & \times |m\rangle|n\rangle\langle m|\langle n|\left(\frac{1}{3}\sum_{\lambda\sigma\kappa}^{x,y,z} \mathbf{T}_{\lambda\sigma\kappa}^{AB}(\mu_{\lambda}^A\theta_{\sigma\kappa}^B - \theta_{\lambda\sigma}^A\mu_{\kappa}^B)\right)|0_A\rangle|0_B\rangle\Bigg\} \\ & /[(E_m^A - E_0^A) + (E_n^B - E_0^B)] \end{aligned} \tag{7}$$

The integrals that involve the charge q may be expressed in the form $\langle 0_A|q^A|m\rangle = q^A\langle 0_A|m\rangle = 0$, since q is a scalar, and the ground and excited states of the same molecule are orthogonal to each other. Hence eq 7 starts from the dipole−dipole term. From eqs 5c and 5d, $\mathrm{T}_{\alpha\beta}$ and $\mathrm{T}_{\gamma\sigma\kappa}$ are of the order R^{-3} and R^{-4},

dx.doi.org/10.1021/ct500017n | J. Chem. Theory Comput. 2014, 10, 1576−1587

respectively. Therefore E7 arises from the second and third terms in eq 7. The first term of eq 7 is the familiar R^{-6} dispersion term. The last term in eq 7 is part of the R^{-8} dispersion term, which will be discussed in a subsequent paper. Collecting the terms for E7 and simplifying the notation by using $E_{m0} = E_m - E_0$ yields

$$\begin{aligned}
\mathrm{E7} = -\sum_{\substack{m\neq 0\\ n\neq 0}} \Bigg\{ & \langle 0_A|\langle 0_B| \sum_{\alpha\beta}^{x,y,z} \mathbf{T}^{AB}_{\alpha\beta}\mu^A_\alpha\mu^B_\beta|m\rangle|n\rangle\langle m|\langle n| \\
& \times \left(\frac{1}{3}\sum_{\gamma\sigma\kappa}^{x,y,z} \mathbf{T}^{AB}_{\gamma\sigma\kappa}(\mu^A_\gamma\theta^B_{\sigma\kappa} - \theta^A_{\gamma\sigma}\mu^B_\kappa)\right)|0_A\rangle|0_B\rangle + \langle 0_A|\langle 0_B| \\
& \times \left(\frac{1}{3}\sum_{\alpha\beta\gamma}^{x,y,z} \mathbf{T}^{AB}_{\alpha\beta\gamma}(\mu^A_\alpha\theta^B_{\beta\gamma} - \theta^A_{\alpha\beta}\mu^B_\gamma)\right)|m\rangle|n\rangle\langle m|\langle n| \\
& \times \sum_{\sigma\kappa}^{x,y,z} \mathbf{T}^{AB}_{\sigma\kappa}\mu^A_\sigma\mu^B_\kappa|0_A\rangle|0_B\rangle\Bigg\}/[(E^A_m - E^A_0) + (E^B_n - E^B_0)] \\
= -\sum_{\substack{m\neq 0\\ n\neq 0}} 2\Bigg\{ & \langle 0_A|\langle 0_B| \sum_{\alpha\beta}^{x,y,z} \mathbf{T}^{AB}_{\alpha\beta}\mu^A_\alpha\mu^B_\beta|m\rangle|n\rangle\langle m|\langle n| \\
& \times \left(\frac{1}{3}\sum_{\gamma\sigma\kappa}^{x,y,z} \mathbf{T}^{AB}_{\gamma\sigma\kappa}(\mu^A_\gamma\theta^B_{\sigma\kappa} - \theta^A_{\gamma\sigma}\mu^B_\kappa)\right)|0_A\rangle|0_B\rangle\Bigg\}/[E^A_{m0} + E^B_{n0}]
\end{aligned} \tag{8}$$

The indices $\alpha, \beta, \gamma, \sigma, \kappa$ all run over the Cartesian coordinates x, y, and z, hence the first and second terms in the first equality of eq 8 are equivalent and may be combined into one term. The **T** tensors are constant at a fixed configuration. Rearranging the integrand yields,

$$\begin{aligned}
E7 = -2\sum_{\alpha\beta\gamma\sigma\kappa}^{x,y,z} T^{AB}_{\alpha\beta}T^{AB}_{\gamma\sigma\kappa} \sum_{\substack{m\neq 0\\ n\neq 0}} \frac{1}{E^A_{m0} + E^B_{n0}} \Bigg[& \langle 0_A|\mu^A_\alpha|m\rangle\langle m|\mu^A_\gamma|0_A\rangle \\
& \times \langle 0_B|\mu^B_\beta|n\rangle\langle n|\frac{1}{3}\theta^B_{\sigma\kappa}|0_B\rangle - \langle 0_A|\mu^A_\alpha|m\rangle\langle m|\frac{1}{3}\theta^A_{\gamma\sigma}|0_A\rangle\langle 0_B|\mu^B_\beta|n\rangle \\
& \times \langle n|\mu^B_\kappa|0_B\rangle\Bigg]
\end{aligned} \tag{9}$$

The denominator of eq 9 is transformed by the Casimir–Polder identity:[9,20]

$$\frac{1}{A+B} = \frac{2}{\pi}\int_0^\infty \frac{AB}{(A^2+\omega^2)(B^2+\omega^2)}d\omega \tag{10}$$

Applying eq 10 to the denominator in eq 9 yields

$$\begin{aligned}
\frac{1}{E^A_{m0} + E^B_{n0}} &= \frac{1}{\hbar}\frac{1}{\omega^A_{m0} + \omega^B_{n0}} \\
&= \frac{2}{\pi}\frac{1}{\hbar}\int_0^\infty d\omega \frac{\omega^A_{m0}\omega^B_{n0}}{[(\omega^A_{m0})^2 + \omega^2][(\omega^B_{n0})^2 + \omega^2]}
\end{aligned} \tag{11}$$

Now the integrand can be written as a product of a term involving only A and a term involving only B:

$$\begin{aligned}
\mathrm{E7} = -2\sum_{\alpha\beta\gamma\sigma\kappa}^{x,y,z} \mathbf{T}^{AB}_{\alpha\beta}\mathbf{T}^{AB}_{\gamma\sigma\kappa}\frac{1}{\hbar}\frac{2}{\pi}\frac{1}{3}\int_0^\infty d\omega \Bigg\{ & \sum_{\substack{m\neq 0\\ n\neq 0}} \left(\frac{\omega^A_{m0}\langle 0_A|\mu^A_\alpha|m\rangle\langle m|\mu^A_\gamma|0_A\rangle}{(\omega^A_{m0})^2 + \omega^2}\right) \\
& \times \left(\frac{\omega^B_{n0}\langle 0_B|\mu^B_\beta|n\rangle\langle n|\theta^B_{\sigma\kappa}|0_B\rangle}{(\omega^B_{n0})^2 + \omega^2}\right) - \sum_{\substack{m\neq 0\\ n\neq 0}} \left(\frac{\omega^A_{m0}\langle 0_A|\mu^A_\alpha|m\rangle\langle m|\theta^A_{\gamma\sigma}|0_A\rangle}{(\omega^A_{m0})^2 + \omega^2}\right) \\
& \times \left(\frac{\omega^B_{n0}\langle 0_B|\mu^B_\beta|n\rangle\langle n|\mu^B_\kappa|0_B\rangle}{(\omega^B_{n0})^2 + \omega^2}\right)\Bigg\}
\end{aligned} \tag{12}$$

From time-dependent perturbation theory, one can express the dynamic dipole–dipole and dipole–quadrupole polarizabilities as, respectively,

$$\alpha_{\alpha\beta}(\omega) = 2\sum_{m\neq 0}\frac{\omega_{m0}\langle 0|\mu_\alpha|m\rangle\langle m|\mu_\beta|0\rangle}{\hbar(\omega^2_{m0} - \omega^2)} \tag{13}$$

$$A_{\alpha,\beta\gamma}(\omega) = 2\sum_{n\neq 0}\frac{\omega_{n0}\langle 0|\mu_\alpha|n\rangle\langle n|\theta_{\beta\gamma}|0\rangle}{\hbar(\omega^2_{n0} - \omega^2)} \tag{14}$$

Since $\omega^2 = -(i\omega)^2$, one can cast the E7 expression in terms of dynamic dipole–quadrupole polarizability tensors over the imaginary frequency range:

$$\begin{aligned}
\mathrm{E7} &= -2\sum_{\alpha\beta\gamma\sigma\kappa}^{x,y,z} \mathbf{T}^{AB}_{\alpha\beta}\mathbf{T}^{AB}_{\gamma\sigma\kappa}\frac{2\hbar}{\pi}\int_0^\infty d\omega\Big\{\frac{1}{3}\times\frac{1}{2}\times\frac{1}{2}\alpha^A_{\alpha\gamma}(i\omega)A^B_{\beta,\sigma\kappa}(i\omega) \\
&\quad - \frac{1}{3}\times\frac{1}{2}\times\frac{1}{2}\alpha^B_{\beta\kappa}(i\omega)A^A_{\alpha,\gamma\sigma}(i\omega)\Big\} \\
&= -\frac{\hbar}{3\pi}\sum_{\alpha\beta\gamma\sigma\kappa}^{x,y,z} \mathbf{T}^{AB}_{\alpha\beta}\mathbf{T}^{AB}_{\gamma\sigma\kappa}\int_0^\infty d\omega[\alpha^A_{\alpha\gamma}(i\omega)A^B_{\beta,\sigma\kappa}(i\omega) - \alpha^B_{\beta\kappa}(i\omega)A^A_{\alpha,\gamma\sigma}(i\omega)]
\end{aligned} \tag{15}$$

The integral in eq 15 is evaluated numerically using a 12-point Gauss-Legendre quadrature. By a change of variable,

$$\omega = \omega_0\frac{1+t}{1-t} \text{ and } d\omega = \frac{2\omega_0}{(1-t)^2}dt \tag{16}$$

the integral in eq 15 becomes

$$\begin{aligned}
&\int_0^\infty d\omega[\alpha^A_{\alpha\gamma}(i\omega)A^B_{\beta,\sigma\kappa}(i\omega) - \alpha^B_{\beta\kappa}(i\omega)A^A_{\alpha,\gamma\sigma}(i\omega)] \\
&= \int_{-1}^1 dt\frac{2\omega_0}{(1-t)^2}[\alpha^A_{\alpha\gamma}(i\omega(t))A^B_{\beta,\sigma\kappa}(i\omega(t)) - \alpha^B_{\beta\kappa}(i\omega(t))A^A_{\alpha,\gamma\sigma}(i\omega(t))] \\
&= \sum_{n=1}^{12} W(n)\frac{2\omega_0}{(1-t_n)^2}[\alpha^A_{\alpha\gamma}(i\omega_n)A^B_{\beta,\sigma\kappa}(i\omega_n) - \alpha^B_{\beta\kappa}(i\omega_n)A^A_{\alpha,\gamma\sigma}(i\omega_n)]
\end{aligned} \tag{17}$$

where $W(n)$ and t_n are the Gauss-Legendre weights and abscissas, which have been determined previously for the R^{-6} term in the dispersion energy.[18,19] The optimal value for ω_0 is found to be 0.3.[21] Now the E7 dispersion energy is

$$\begin{aligned}
\mathrm{E7} = -\frac{\hbar}{3\pi}\sum_{\alpha\beta\gamma\sigma\kappa}^{x,y,z} \mathbf{T}^{AB}_{\alpha\beta}\mathbf{T}^{AB}_{\gamma\sigma\kappa}\sum_{n=1}^{12} W(n)\frac{2\omega_0}{(1-t_n)^2} \\
\times [\alpha^A_{\alpha\gamma}(i\omega_n)A^B_{\beta,\sigma\kappa}(i\omega_n) - \alpha^B_{\beta\kappa}(i\omega_n)A^A_{\alpha,\gamma\sigma}(i\omega_n)]
\end{aligned} \tag{18}$$

A distributed multipole expansion model of the molecule has the advantages that one attains improved convergence properties and a better description of the molecular charge distribution.[9,14,22] In particular for dispersion, a distributed treatment portrays a more realistic picture of the response of

dx.doi.org/10.1021/ct500017n | J. Chem. Theory Comput. 2014, 10, 1576–1587

the molecule from nonuniform fields due to other molecular systems.

If one divides the molecule into "regions", each described by its own multipole expansion with its own origin, the interaction operator V has the form:[9,23,24]

$$\hat{V} = \sum_{a\in A}\sum_{b\in B}\left[\mathbf{T}^{ab}q^a q^b + \mathbf{T}^{ab}_{\alpha}(q^a\mu^b_\alpha - \mu^a_\alpha q^b) + \mathbf{T}^{ab}_{\alpha\beta}\left(\frac{1}{3}q^a\theta^b_{\alpha\beta} - \mu^a_\alpha\mu^b_\beta + \frac{1}{3}\theta^a_{\alpha\beta}q^b\right) + ...\right] \tag{19}$$

The double sum runs over the expansion centers a of molecule A and b of molecule B. The $\mathbf{T}^{ab}$ are the electrostatic tensors between two expansion centers a and b. Note that the Einstein convention, the repeated-subscript summation convention, is used here for Cartesian coordinates (suffix) to avoid cumbersome equations. Substituting eq 19, truncated at the dipole−quadrupole term, into eq 2 and combining with eq 6 gives eq 20:

$$\begin{aligned}
E^{disp} &= -\sum_{\substack{m\neq 0\\ n\neq 0}}\sum_{a,c\in A}\sum_{b,d\in B}\frac{\left\{\begin{array}{l}\langle 0_A|\langle 0_B|T^{ab}_{\alpha\beta}\mu^a_\alpha\mu^b_\beta|m\rangle|n\rangle\langle m|\langle n|T^{cd}_{\gamma\sigma}\mu^c_\gamma\mu^d_\sigma|0_A\rangle|0_B\rangle\\ +\langle 0_A|\langle 0_B|T^{ab}_{\alpha\beta}\mu^a_\alpha\mu^b_\beta|m\rangle|n\rangle\langle m|\langle n|\frac{1}{3}T^{cd}_{\gamma\sigma\kappa}(\mu^c_\gamma\theta^d_{\sigma\kappa} - \theta^c_{\gamma\sigma}\mu^d_\kappa)|0_A\rangle|0_B\rangle\\ +\langle 0_A|\langle 0_B|\frac{1}{3}T^{ab}_{\alpha\beta\gamma}(\mu^a_\alpha\theta^b_{\beta\gamma} - \theta^a_{\alpha\beta}\mu^b_\gamma)|m\rangle|n\rangle\langle m|\langle n|T^{cd}_{\sigma\kappa}\mu^c_\sigma\mu^d_\kappa|0_A\rangle|0_B\rangle\\ +\langle 0_A|\langle 0_B|\frac{1}{3}T^{ab}_{\alpha\beta\gamma}(\mu^a_\alpha\theta^b_{\beta\gamma} - \theta^a_{\alpha\beta}\mu^b_\gamma)|m\rangle|n\rangle\langle m|\langle n|\frac{1}{3}T^{cd}_{\lambda\sigma\kappa}(\mu^c_\lambda\theta^d_{\sigma\kappa} - \theta^c_{\lambda\sigma}\mu^d_\kappa)|0_A\rangle|0_B\rangle\end{array}\right\}}{E^A_{m0}+E^B_{n0}}\\
&= -\sum_{\substack{m\neq 0\\ n\neq 0}}\sum_{a,c\in A}\sum_{b,d\in B}\frac{\{T^{ab}_{\alpha\beta}T^{cd}_{\gamma\sigma}\langle 0_A|\mu^a_\alpha|m\rangle\langle 0_B|\mu^b_\beta|n\rangle\langle m|\mu^c_\gamma|0_A\rangle\langle n|\mu^d_\sigma|0_B\rangle\}}{E^A_{m0}+E^B_{n0}}\\
&\quad -\sum_{\substack{m\neq 0\\ n\neq 0}}\sum_{a,c\in A}\sum_{b,d\in B}\frac{1}{3}\frac{\left\{\begin{array}{l}T^{ab}_{\alpha\beta}T^{cd}_{\gamma\sigma\kappa}\langle 0_A|\mu^a_\alpha|m\rangle\langle 0_B|\mu^b_\beta|n\rangle\langle m|\mu^c_\gamma|0_A\rangle\langle n|\theta^d_{\sigma\kappa}|0_B\rangle\\ -T^{ab}_{\alpha\beta}T^{cd}_{\gamma\sigma\kappa}\langle 0_A|\mu^a_\alpha|m\rangle\langle 0_B|\mu^b_\beta|n\rangle\langle m|\theta^c_{\gamma\sigma}|0_A\rangle\langle n|\mu^d_\kappa|0_B\rangle\\ +T^{ab}_{\alpha\beta\gamma}T^{cd}_{\sigma\kappa}\langle 0_A|\mu^a_\alpha|m\rangle\langle 0_B|\theta^b_{\beta\gamma}|n\rangle\langle m|\mu^c_\sigma|0_A\rangle\langle n|\mu^d_\kappa|0_B\rangle\\ -T^{ab}_{\alpha\beta\gamma}T^{cd}_{\sigma\kappa}\langle 0_A|\theta^a_{\alpha\beta}|m\rangle\langle 0_B|\mu^b_\gamma|n\rangle\langle m|\mu^c_\sigma|0_A\rangle\langle n|\mu^d_\kappa|0_B\rangle\end{array}\right\}}{E^A_{m0}+E^B_{n0}}\\
&\quad -\sum_{\substack{m\neq 0\\ n\neq 0}}\sum_{a,c\in A}\sum_{b,d\in B}\frac{1}{9}\frac{\left\{T^{ab}_{\alpha\beta\gamma}T^{cd}_{\gamma\sigma\kappa}\left[\begin{array}{l}\langle 0_A|\mu^a_\alpha|m\rangle\langle 0_B|\theta^b_{\beta\gamma}|n\rangle\langle m|\mu^c_\lambda|0_A\rangle\langle n|\theta^d_{\sigma\kappa}|0_B\rangle\\ -\langle 0_A|\theta^a_{\alpha\beta}|m\rangle\langle 0_B|\mu^b_\gamma|n\rangle\langle m|\mu^c_\lambda|0_A\rangle\langle n|\theta^d_{\sigma\kappa}|0_B\rangle\\ -\langle 0_A|\mu^a_\alpha|m\rangle\langle 0_B|\theta^b_{\beta\gamma}|n\rangle\langle m|\theta^c_{\lambda\sigma}|0_A\rangle\langle n|\mu^d_\kappa|0_B\rangle\\ +\langle 0_A|\theta^a_{\alpha\beta}|m\rangle\langle 0_B|\mu^b_\gamma|n\rangle\langle m|\theta^c_{\lambda\sigma}|0_A\rangle\langle n|\mu^d_\kappa|0_B\rangle\end{array}\right]\right\}}{E^A_{m0}+E^B_{n0}}
\end{aligned} \tag{20}$$

Each term in the second equality of eq 20 can be symbolically represented as

$$\sum_{\substack{m\neq 0\\ n\neq 0}}\sum_{a,c\in A}\sum_{b,d\in B}\frac{\mathbf{T}^{ab}\mathbf{T}^{cd}Q^aQ^cQ^bQ^d}{E_{m0}+E_{n0}} \tag{21}$$

In eq 21 Q^a symbolizes the integral of a multipole moment expanded about the center a. By going through the same derivation as the single-expansion center model, the dispersion energy calculated using the distributed model can be symbolically represented as

$$\begin{aligned}
E_{\text{disp}} &= \frac{1}{\hbar}\frac{2}{\pi}\sum_{\substack{m\neq 0\\ n\neq 0}}\sum_{a,c\in A}\sum_{b,d\in B}\int_0^\infty d\omega\frac{\omega^A_{m0}\omega^B_{n0}T^{ab}T^{cd}Q^aQ^cQ^bQ^d}{[(\omega^A_{m0})^2+\omega^2][(\omega^B_{n0})^2+\omega^2]}\\
&= \frac{1}{\hbar}\frac{2}{\pi}\sum_{a,c\in A}\sum_{b,d\in B}\mathbf{T}^{ab}\mathbf{T}^{cd}\int_0^\infty d\omega\left(\sum_{m\neq 0}\frac{\omega^A_{m0}Q^aQ^c}{[(\omega^A_{m0})^2+\omega^2]}\right)\\
&\quad\times\left(\sum_{n\neq 0}\frac{\omega^B_{n0}Q^bQ^d}{[(\omega^B_{n0})^2+\omega^2]}\right)
\end{aligned} \tag{22}$$

Note that the two $\mathbf{T}$ tensors in eq 22 can now be different from each other. The terms in large brackets in the second equality in eq 22 have the form of a multipole−multipole dynamic polarizability tensor $\mathbf{P}$ [eq 23]. The two multipole moments in eq 23 do not necessarily have the same expansion centers (that is, a can be different from c).

$$\mathbf{P}^{ac} = \sum_{m\neq 0}\frac{\omega^A_{m0}Q^aQ^c}{[(\omega^A_{m0})^2+\omega^2]} \tag{23}$$

Stone and Tong[23] termed the polarizability with the same expansion center ($a = c$) as 'local'. If the expansion centers differ ($a \neq c$), the polarizability is termed 'nonlocal'. The nonlocal polarizability arises naturally from a distributed formulation in which a field in one region causes a response in another region of the same molecule. Stone and Tong have shown, in spherical tensor formalism, that the nonlocal multipole−multipole polarizability can be transformed into the local form by a shifting procedure provided that the centers of the moments are not moved too far. This shifting procedure transforms the dispersion energy expression to a familiar site−site description:

$$\begin{aligned}
E_{\text{disp}} &= \frac{1}{\hbar}\frac{2}{\pi}\sum_{a\in A}\sum_{b\in B}\mathbf{T}^{ab}\mathbf{T}^{c\to a,d\to b}\int_0^\infty d\omega\left(\sum_{m\neq 0}\frac{\omega^A_{m0}Q^aQ^{c\to a}}{[(\omega^A_{m0})^2+\omega^2]}\right)\\
&\quad\times\left(\sum_{n\neq 0}\frac{\omega^B_{n0}Q^bQ^{d\to b}}{[(\omega^B_{n0})^2+\omega^2]}\right)\\
&= \frac{1}{\hbar}\frac{2}{\pi}\sum_{a\in A}\sum_{b\in B}\mathbf{T}^{ab}\mathbf{T}^{ab}\int_0^\infty d\omega\mathbf{P}^a\mathbf{P}^b
\end{aligned} \tag{24}$$

dx.doi.org/10.1021/ct500017n | J. Chem. Theory Comput. 2014, 10, 1576−1587

$Q^{c\to a}$ and $Q^{d\to b}$ symbolize the multipole moments whose centers have been shifted. This shifting treatment is formally exact at sufficiently long-range. Stone and Tong have demonstrated that <2% error is incurred for small systems using the shifted formula.[23]

In the EFP method, each LMO is taken to be a distributed "region", and naturally the LMO centroids are chosen as the expansion centers. Jensen and Gordon[25] introduced and implemented the localized charge distribution (LCD) method[26−32] for Hartree-Fock wave functions, in which the key idea is to partition the nuclear charge and assign part of the nuclear charge to a particular LMO predominantly associated with that nucleus. This "local" nuclear charge and the electrons in the LMO together constitute an electrically neutral LCD. The dipole moments of such neutral localized charge distributions are invariant with respect to the shifting. Consequently the dipole−dipole polarizability is the same before and after the shift. For the dipole−quadrupole polarizability, one can shift the origin of the dipole moment to coincide with the origin of the quadrupole moment, and again this gives an LMO dipole−quadrupole polarizability that is identical to that before the shift. Thus, the polarizabilities that are relevant to E7 are unchanged, and a distributed E7 expression without the nonlocal polarizabilities can be easily written. The E7 derived from the distributed multipole expansion at the centroids of LMOs is

$$\mathrm{E7(LMO)} = -\frac{1}{3}\frac{\hbar}{\pi}\sum_{k\in A}^{\mathrm{LMO}}\sum_{j\in B}^{\mathrm{LMO}}\sum_{\alpha\beta\gamma\sigma\kappa}^{x,y,z}\mathbf{T}^{kj}_{\alpha\beta}\mathbf{T}^{kj}_{\gamma\sigma\kappa}\int_0^\infty d\omega \times [\alpha^k_{\alpha\gamma}(i\omega)A^j_{\beta,\sigma\kappa}(i\omega) - \alpha^j_{\beta\kappa}(i\omega)A^k_{\alpha,\gamma\sigma}(i\omega)] \tag{25}$$

where α^k is the dipole−dipole dynamic polarizability of the kth LMO expanded at its centroid. Similarly, A^j is the dipole−quadrupole dynamic polarizability of the jth LMO expanded at its centroid. This E7 dispersion energy is called E7 (LMO), to distinguish it from E7 calculated using molecular polarizabilities, which is called E7 (molecular).

The molecular dynamic polarizability can be partitioned into LMO contributions:

$$P^A(\omega) = \sum_{l\in A}^{\mathrm{LMO}} P^A_l(\omega) \tag{26}$$

The decomposition is always valid for polarizabilities of any rank when the LMO polarizabilities use the same expansion center as the molecular polarizability. For the dipole−dipole polarizability, the dipole moments are invariant with respect to the origins as discussed above. So the LMO dynamic dipole polarizability that is obtained at the center of mass is equal to the LMO polarizability obtained at the centroids of the LMOs. However, the quadrupole moments are origin dependent, which means the LMO dynamic dipole−quadrupole polarizability expanded at the centroids of the LMOs will be different from those expanded at the center of mass. The dipole−quadrupole polarizabilities obtained using different origins are related through the following transformation:

$$A'^{l}_{\alpha,\beta\gamma} = A^l_{\alpha,\beta\gamma} - \left(\frac{3}{2}r'_\beta\alpha^l_{\gamma\alpha} + \frac{3}{2}r'_\gamma\alpha^l_{\alpha\beta} - \sum_\kappa r'_\kappa\alpha^l_{\kappa\alpha}\delta_{\beta\gamma}\right) \tag{27}$$

where r' is the shift of the origin from the center of mass to the centroid of the lth LMO. A^l and $A'^l$are the dynamic LMO dipole−quadrupole polarizabilities expanded at the center of mass and the centroid of LMO l, respectively.

Renaming the transformed LMO dipole−quadrupole polarizability as A^l (i.e., dropping the superscript prime), substituting the transformed A^l into eq 25 and applying the same Gauss-Legendre numerical integration procedure, the final distributed E7 expression becomes

$$E7(\mathrm{LMO}) = -\frac{1}{3}\frac{\hbar}{\pi}\sum_{k\in A}^{\mathrm{LMO}}\sum_{j\in B}^{\mathrm{LMO}}\sum_{\alpha\beta\gamma\sigma\kappa}^{x,y,z}\mathbf{T}^{kj}_{\alpha\beta}\mathbf{T}^{kj}_{\gamma\sigma\kappa}\sum_{n=1}^{12}W(n)\frac{2\omega_0}{(1-t_n)^2} \times [\alpha^k_{\alpha\gamma}(i\omega_n)A^j_{\beta,\sigma\kappa}(i\omega_n) - \alpha^j_{\beta\kappa}(i\omega_n)A^k_{\alpha,\gamma\sigma}(i\omega_n)] \tag{28}$$

To calculate the LMO dynamic dipole−quadrupole polarizability, the approach described by Champagne et al is followed.[33] The response is calculated in the same way as in the dipole−dipole case.[10,18]

$$(\mathbf{H}^{(2)}\mathbf{H}^{(1)} - (i\nu)^2)Z = -\mathbf{H}^{(2)}P \tag{29}$$

$\mathbf{H}^{(1)}$ is the real orbital Hessian matrix.

$$\mathbf{H}^{(1)}_{aibj} = (\varepsilon_a - \varepsilon_i)\delta_{ab}\delta_{ij} + 4(ai|bj) - (ab|ij) - (aj|bi) \tag{30}$$

where ε_i and ε_a are the occupied and virtual Hartree−Fock orbital energies, respectively, and $(ai|bj)$, etc., are the two-electron integrals over the molecular orbital basis. $\mathbf{H}^{(2)}$ is used to calculate the magnetizability and is defined as

$$\mathbf{H}^{(2)}_{aibj} = (\varepsilon_a - \varepsilon_i)\delta_{ab}\delta_{ij} + (ab|ij) - (aj|bi) \tag{31}$$

P in eq 29 is the perturbation and, in this case, is the dipole moment matrix,

$$\mathbf{P}_{ai} = \langle\phi_a|\hat{\mu}|\phi_i\rangle \tag{32}$$

Once the response matrix $\mathbf{Z}$ is obtained, it is combined with the quadrupole moment integrals to form the dipole−quadrupole polarizability.

$$A_{\alpha,\beta\gamma}(i\nu) = \sum_{ai} 2\langle\phi^a|\hat{\theta}_{\beta\gamma}|\phi^i\rangle\mathbf{Z}^{ai}_\alpha(i\nu) \tag{33}$$

where the subscripts run over Cartesian coordinates and the superscripts i and a refer to the occupied and virtual orbital indices, respectively. Eq 33 gives the molecular dipole−quadrupole polarizability at the center of mass. The dipole−quadrupole contribution from the l^{th} LMO is obtained by transforming the canonical occupied orbitals to localized orbitals and summing over only the virtual orbitals.

$$A^l_{\alpha,\beta\gamma}(i\nu) = \sum_a^{\mathrm{vir}} 2\Big(\sum_i^{\mathrm{occ}}\langle\phi^a|\hat{\theta}_{\beta\gamma}|\phi^i\rangle\mathbf{T}^{il}\Big)\Big(\sum_i^{\mathrm{occ}}\mathbf{Z}^{ai}_\alpha(i\nu)\mathbf{T}^{il}\Big) \tag{34}$$

Then the origin shift as in eq 27 is carried out to yield the LMO dipole−quadrupole polarizability at the respective centroid.

As for the R^{-6} contribution to the dispersion energy, a damping function is necessary for E7 to have the correct asymptotic behavior as R approaches zero. Both Tang−Toennies[34] and overlap-based[35] damping functions have been derived. The Tang−Toennies damping function for E7 has the form:

$$f_7^{TT}(R) = 1 - \left(\sum_{k=0}^{7}\frac{(bR)^k}{k!}\right)\exp(-bR) \tag{35}$$

where the parameter b was previously chosen to be 1.5 for the E6 term.[18,35] The overlap-based damping function for E7 is

$$f_7^{\mathbf{S}} = 1 - \mathbf{S}^2 \sum_{n=0}^{3} \frac{(-2\ln|\mathbf{S}|)^n}{n!}$$
$$= 1 - \mathbf{S}^2\left(1 + (-2\ln|\mathbf{S}|) + \frac{(-2\ln|\mathbf{S}|)^2}{2!} + \frac{(-2\ln|\mathbf{S}|)^3}{3!}\right) \quad (36)$$

where $\mathbf{S}$ is the matrix of the intermolecular overlap integrals over the LMOs.

Codes have been implemented into the GAMESS[36,37] software package to compute the dynamic molecular dipole−dipole and dipole−quadrupole polarizabilities expanded at the center of mass of the molecule, the dynamic LMO dipole−quadrupole polarizability expanded at the center of mass of the molecule, the origin shift from the center of mass to the LMO centroids for the LMO dipole−quadrupole polarizability, E7 using the molecular polarizability (eq 15) and using the distributed LMO polarizability (eq 25), overlap-based and Tang−Toennies damping functions, and auxiliary subroutines that write and read the dynamic polarizabilities.

The anisotropic R^{-6} dispersion interaction obtained from the molecular and LMO dipole−dipole polarizability, E6 (molecular) and E6 (LMO), respectively, have previously been derived:[18,19]

$$\mathrm{E6(molecular)} = -\frac{\hbar}{2\pi} \sum_{\alpha\beta\sigma\lambda}^{x,y,z} \mathbf{T}_{\alpha\beta}^{AB}\mathbf{T}_{\sigma\lambda}^{AB} \times \int_0^\infty \alpha_{\alpha\sigma}^{A}(i\omega)\alpha_{\beta\lambda}^{B}(i\omega)d\omega \quad (37)$$

$$\mathrm{E6(LMO)} = -\frac{\hbar}{2\pi} \sum_{k\in A}^{\mathrm{LMO}} \sum_{j\in B}^{\mathrm{LMO}} \sum_{\alpha\beta\sigma\lambda}^{x,y,z} \mathbf{T}_{\alpha\beta}^{kj}\mathbf{T}_{\sigma\lambda}^{kj} \times \int_0^\infty \alpha_{\alpha\sigma}^{k}(i\omega)\alpha_{\beta\lambda}^{j}(i\omega)d\omega \quad (38)$$

These anisotropic E6 expressions have been implemented in GAMESS as well to illustrate the comparisons of the R^{-6} and R^{-7} dispersion interaction in this study.

III. COMPUTATIONAL DETAILS

There are relatively few E7 calculations for molecules of arbitrary geometry in the literature, although explicit orientation-dependent E7 expressions have been developed[38] for simple systems such as a pair of linear molecules. Magnasco and co-workers have done a series of studies on the LiH−LiH system in which they calculated full-CI quality, imaginary frequency-dependent dipole−dipole and dipole−quadrupole polarizabilities for ground-state LiH and C_6 and C_7 dispersion coefficients for LiH−LiH.[39−42] The angle-dependent C_n dispersion coefficients for two linear molecules are[38−42]

$$C_n(\theta_A, \theta_B, \varphi) = \sum_{L_A L_B M} C_n^{L_A L_B M} P_{L_A}^{M}(\cos\theta_A) P_{L_B}^{M}(\cos\theta_B)\cos M\varphi$$
$$n = l_a + l_a' + l_b + l_b' + 2, \quad 0 \le M \le \min(L_A, L_B)$$
$$|l_a - l_a'| \le L_A \le l_a + l_a', \quad |l_b - l_b'| \le L_B \le l_b + l_b' \quad (39)$$

The relative orientation of two LiH molecules is schematically illustrated in Figure 1 in which θ_A, θ_B, and φ are the angles that specify the relative orientation. The angle θ varies from 0 to π, and the angle φ varies from 0 to 2π. In Figure 1, the increments in φ were taken to be $\pi/4$ l specifies the angular momentum

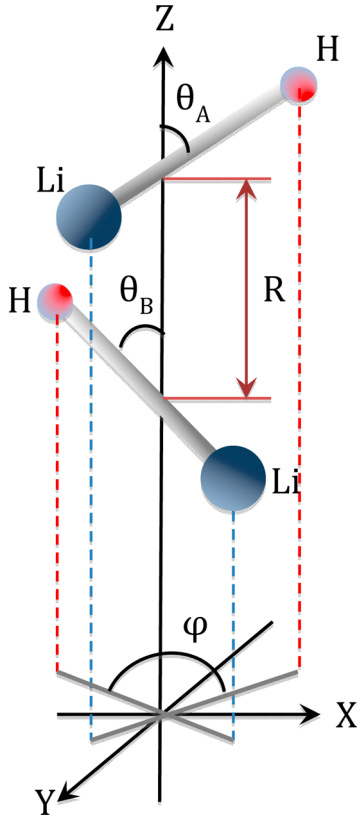

Figure 1. A schematic representation of LiH−LiH dimer. The LiH molecules intersect with the Z-axis at their centers of mass. R is the distance between the two centers of mass, which is set to 10 Bohr in this study.

quantum numbers of A and B. L_A and L_B are the resultant total angular momentum L of molecule A and molecule B, respectively. The P_L^M in eq 39 are the associated Legendre polynomials. The coefficient, $C_n^{L_A L_B M}$, is best expressed in terms of irreducible dispersion constants, which are linear combinations of elementary dispersion constants $C_{ab} = (1/2\pi)\int_0^\infty du\alpha_a(iu)\alpha_b(iu)$, where $a = l_a l_a' m$ and $b = l_b l_b' m$ are labels specifying polarizabilities in spherical tensor form. Given the $C_7^{L_A L_B M}$,[40,42] an in-house Python program was written to generate LiH−LiH dimers of various relative orientations and to calculate $C_7(\theta_A,\theta_B,\varphi)$ and consequently E7 = C_7/R^7. R is the distance between the centers of mass of the two LiH molecules and is kept at 10 Bohr to ensure negligible overlap. The E7 values obtained in this manner are taken as the reference (benchmark) values against which the EFP E7 values will be compared. The E7 (benchmark) values can be directly compared with the EFP E7 (molecular) values since the center of mass is the EFP molecular polarizability expansion center and defines the EFP **T** tensors.

The molecular dynamic polarizabilities over the imaginary frequency range are computed in a preparatory time-dependent Hartree−Fock calculation in GAMESS with the 6-311++G(3df,2p) basis set. In the next section, E7 (molecular) is compared directly to the E7 (benchmark). The distributed LMO polarizabilities over the same imaginary frequency range are generated with the same 6-311++G(3df,2p) basis set, and the expansion centers are shifted to the LMO centroids. The distributed E7, E7 (LMO), is calculated according to eq 25.

dx.doi.org/10.1021/ct500017n | J. Chem. Theory Comput. 2014, 10, 1576−1587

E6 (molecular), E7 (molecular), E6 (LMO), and E7 (LMO) as well as the isotropic E6 (molecular) and E6 (LMO) have also been calculated for the following dimer systems: Ar, H_2, HF, water, ammonia, methane, methanol, and dicholoromethane. The equilibrium geometries of these dimer systems are taken from the previous study of the EFP−ab initio dispersion interaction.[19] All of the monomer EFP potentials are generated with the 6-311++G(3df,2p) basis set except methanol (6-311++G(2d,2p)) and dicholoromethane (6-31+G(d)). The symmetry-adapted perturbation theory (SAPT) calculations for these two systems were carried out using the smaller basis sets due to computational cost. The EFP potential energy curves, both E7 (LMO) alone and E6 (LMO) + E7 (LMO), have been generated for $(H_2O)_2$ and $(CH_4)_2$ by varying the intermolecular (center of mass to center of mass) distance from −0.8 to 0.8 Å, in increments of 0.2 Å, with respect to the equilibrium distance. Two damped potential energy curves, using the Tang−Toennies and overlap-based damping functions have also been generated. The E6 (LMO) + E7 (LMO) curves are compared to SAPT[43] dispersion energies, which are available from previous studies.[19] All of the calculations described above were performed with the GAMESS software package.[36,37]

IV. RESULTS AND DISCUSSION

By systematically varying θ_A, θ_B, and φ as described in Section III, a total of 200 different configurations of LiH−LiH dimers were generated. The E7 (molecular) values for these configurations, calculated using the molecular dipole−dipole and dipole−quadrupole polarizabilities expanded about the center of mass of the individual LiH molecules are compared in Table S1 to the E7 (benchmark) results by calculating the ratio E7 (molecular)/ E7 (benchmark). The agreement is excellent, with an average ratio of ∼93% and a standard deviation of ∼4%. The deviation is most likely attributable to the fact that EFP polarizabilities are generated using time dependent Hartree−Fock in which only CIS excited states are included. In contrast, the polarizabilities in refs 29 and 30 are based on full configuration interaction (FCI). For configurations with parallel LiH ($\theta_A = \theta_B$), both E7 (benchmark) and E7 (molecular) are numerically tiny and are considered to be zero with an undefined ratio.

To better illustrate the E7 (molecular) trends Figures 2 and 3 are plotted using selected data from Table S1. LiH−LiH E7 (molecular) depends on the three angles, θ_A, θ_B, φ. To examine the φ dependence, E7 (molecular) values for fixed θ_A and θ_B are plotted in Figure 2 as a function of φ. In Figure 2, $\theta_A = \pi/4$ is chosen as a representative example, and each line represents E7 (molecular) for a particular value of θ_B. As φ varies, E7 is almost constant for a particular θ_A and θ_B combination. Other θ_A and θ_B combinations behave similarly. It is also interesting to note that E7, unlike E6, can be either attractive or repulsive. From Figure 2 it can also be seen that E7 is quite sensitive to changes in θ_B. This observation is much more apparent in Figure 3. Knowing that E7 is rather insensitive to variations of φ, Figure 3 presents E7 with respect to changes of θ_A for fixed $\varphi = 0$. Each curve represents a different θ_B angle. As θ_A varies, the order of magnitude of E7 changes substantially, and in some cases, the sign also changes. Similar curves are obtained for varying θ_B with fixed θ_A.

By examining the numbers in Figure 3 and Table 1, some interesting observations may be made: The configurations that are symmetric about the lower left to upper right diagonal line,

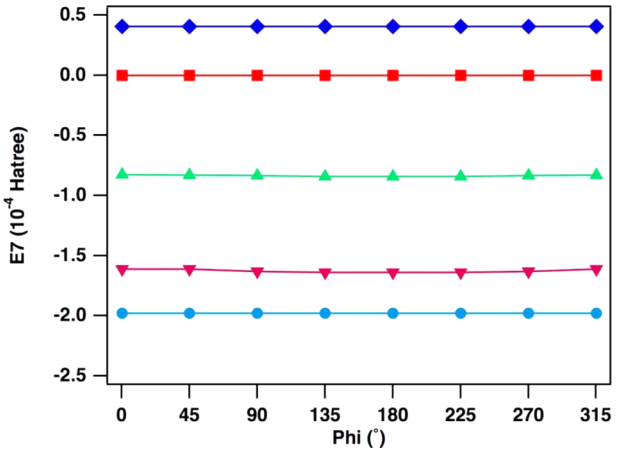

Figure 2. E7 (in 10^{-4} Hartree) as a function of the angle φ, calculated from dynamic molecular polarizabilities over the imaginary frequency range for LiH−LiH dimer with $\theta_A = \pi/4$, θ_B varying from 0 to π and φ from 0 to 2π, in increments of $\pi/4$, from the top to the bottom lines.

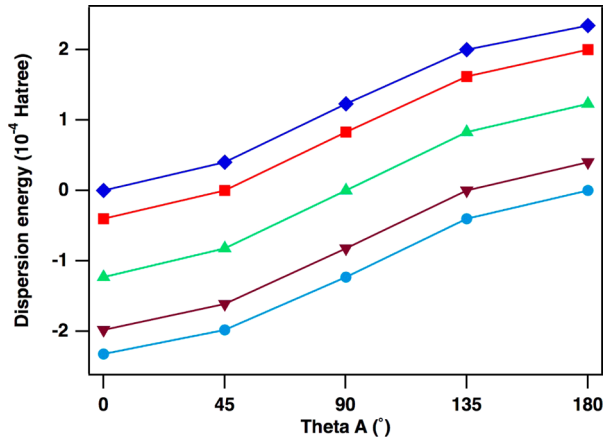

Figure 3. E7 (in 10^{-4} Hartree) as a function of the angle θ_A, calculated from dynamic molecular polarizabilities over the imaginary frequency range for LiH−LiH dimer with $\varphi = 0$, θ_B varying from 0 to π in increments of $\pi/4$, from the top to the bottom lines.

$(\theta_A, \theta_B, \varphi)$ and $(\pi - \theta_B, \pi - \theta_A, \varphi)$, have identical E7. This is expected since they are merely the mirror image of each other. The configurations that are symmetric about the upper left to lower right diagonal line have E7s that are approximately equal in magnitude (difference <1%) and opposite in sign. Such a relationship is expected from eq 39 and is verified by EFP calculations. These symmetry relationships are maintained for other values of φ and give rise to a rotationally averaged E7 (molecular) of zero.

A direct comparison for E7 (LMO) is difficult. Most distributed models use atomic polarizabilities that will (incorrectly) give a zero distributed E7. The centroid of the valence LMO of LiH does not coincide with its center of mass, and therefore an E7 calculated using LMOs does not necessarily equal the E7 based on the molecular polarizability. However, it can be proved (see Appendix) that if the origins of the two interacting molecules are shifted uniformly, that is, in same direction and magnitude, E7 is invariant. This provides a way to check the origin shift implementation and the implementation for calculating E7 (LMO): Instead of shifting the expansion centers of the LMO polarizability from the center of mass to the LMO centroids, one can shift the

dx.doi.org/10.1021/ct500017n | J. Chem. Theory Comput. 2014, 10, 1576−1587

Table 1. E7 (molecular) (in Hartree) Calculated from Dynamic Molecular Polarizabilities over the Imaginary Frequency Range for LiH−LiH Dimer[a]

θ_B \ θ_A	0	π/4	π/2	3π/4	π
0	1.09E-56	4.04E-05	1.23E-04	2.00E-04	2.34E-04
π/4	-4.04E-05	1.18E-15	8.28E-05	1.62E-04	2.00E-04
π/2	-1.23E-04	-8.25E-05	-8.66E-21	8.28E-05	1.23E-04
3π/4	-1.98E-04	-1.61E-04	-8.25E-05	5.38E-16	4.04E-05
π	-2.32E-04	-1.98E-04	-1.23E-04	-4.04E-05	-3.88E-55

[a]For $\varphi = 0$, θ_A (the x-axis) and θ_B (the y-axis) varying from 0 to π, in increments of $\pi/4$.

expansion centers to an arbitrary point such that the shifting vectors are the same for the two interacting molecules. Then the E7 calculated from the molecular polarizability and the E7 calculated from this "arbitrarily" distributed polarizability should match. This indeed is the case for all of the configurations of LiH−LiH dimers assessed in this study.

Table 2 presents E7 (molecular) and E7 (LMO) computed for various dimer systems at their equilibrium configurations. Note that for Ar, the molecular dipole−quadrupole polarizability is the atomic dipole−quadrupole polarizability. Since an atom is centrosymmetric, its dipole−quadrupole polarizability is zero, and consequently its E7 (molecular) is also zero. However, atomic LMOs do not necessarily possess an inversion center. Hence the LMO dipole−quadrupole polarizability of Ar atom is not zero, nor is E7 (LMO). The molecule H_2 contains an inversion center that also coincides with the H_2 LMO inversion center. It is expected that both molecular and LMO dipole−quadrupole polarizability tensors are zero, which give zero E7 (molecular) and E7 (LMO). In some cases, E7 (molecular) and E7 (LMO) can have different signs, reflecting the fact that different multipole expansions give different descriptions of the potential at a truncated finite order. E6 (molecular) and E6 (LMO) as well as their isotropic counterparts for these dimer systems are also computed and shown in Table 2. The isotropic E6 (molecular) deviate very little from the anisotropic E6 (molecular). For the distributed model, the deviations between isotropic and anisotropic E6 (LMO) are comparatively larger, although the absolute deviation is still <0.5 kcal/mol. This validates the isotropic approximation. At the equilibrium configurations of these dimer systems, E7 values (both the molecular and the distributed) are typically only a small fraction of the E6 values, although their signs can be different. For $(H_2O)_2$ and $(NH_3)_2$, E7 values are ∼50% of E6 values and opposite in sign. When the sums E6 + E7 are compared to the SAPT values, the errors are still relatively large, indicating that the series in eq 1 is not converged at the R^{-7} term, and at least the R^{-8} dispersion term is necessary.

One interesting observation is that the dispersion contributions calculated from molecular and LMO polarizabilities can be strikingly different. For example, E6 (LMO) for H_2O and NH_3 dimers are more than double the corresponding E6 (molecular) values. E7 (LMO) and E7 (molecular) can also be rather different. In some cases, E7 (molecular) and E7 (LMO) have different signs, not surprising since the E7 sign is not always negative. To illustrate how these differences arise, consider the simplest case, isotropic E6 (LMO) and E6 (molecular):[18,19]

$$\text{isotropic E6(molecular)} = \frac{C_6^{AB}}{R_{AB}^6} = \frac{\alpha^A\alpha^B}{R_{AB}^6} = \frac{(\sum_{k\in A}\alpha^k)(\sum_{l\in B}\alpha^l)}{R_{AB}^6} = \sum_{kl}^{\text{LMO}}\frac{\alpha^k\alpha^l}{R_{AB}^6} = \sum_{kl}^{\text{LMO}}\frac{C_6^{kl}}{R_{AB}^6} \tag{40}$$

$$\text{isotropic E6(LMO)} = \sum_{kl}^{\text{LMO}}\frac{C_6^{kl}}{R_{kl}^6} = \sum_{kl}^{\text{LMO}}\frac{\alpha^k\alpha^l}{R_{kl}^6} \tag{41}$$

where $\alpha = (1/3)(\alpha_{xx} + \alpha_{yy} + \alpha_{zz})$ is the isotropic dynamic dipole−dipole polarizability. Since the dipole−dipole polarizability is invariant with respect to the origin shift, the molecular dipole−dipole polarizability can be partitioned into LMO contributions exactly (see eq 26). Consequently, the dispersion coefficient C_6^{AB} can be partitioned into C_6^{kl} contributions. The difference between the two E6 expressions in eqs 40 and 41 comes from the difference between R_{AB} and R_{kl}. R_{AB} is the distance between the centers of mass of A and B. R_{kl} is the distance between the centroids of LMOs k and l,

Table 2. E6 (molecular), E7 (molecular), E6 (LMO), and E7 (LMO) for Various Dimer Systems at Their Equilibrium Distances, in kcal/mol[a]

	SAPT	E6 (molecular)	E6 (molecular) (isotropic)	E7 (molecular)	E6 (LMO)	E6 (LMO) (isotropic)	E7 (LMO)
2Ar	−0.390	−0.265	−0.265	0.000	−0.285	−0.295	0.002
$2H_2$	−0.087	−0.058	−0.057	0.000	−0.058	−0.057	0.000
2HF	−1.661	−0.527	−0.499	−0.138	−0.777	−0.661	−0.059
$2H_2O$	−2.191	−0.787	−0.788	−0.107	−1.554	−1.095	0.573
$2NH_3$	−1.909	−0.736	−0.739	−0.046	−1.526	−1.111	0.718
$2CH_4$	−0.736	−0.415	−0.415	0.002	−0.509	−0.570	0.010
2MeOH	−2.253	−0.960	−0.944	0.641	−1.476	−1.252	0.373
$2CH_2Cl_2$	−2.074	−1.197	−1.314	−0.022	−1.802	−1.913	0.421

[a]Isotropic E6 (molecular) and isotropic E6 (LMO) values calculated from LMO dipole polarizabilities are also presented. The SAPT dispersion + exchange dispersion values are listed here as well.

dx.doi.org/10.1021/ct500017n | J. Chem. Theory Comput. 2014, 10, 1576−1587

respectively. By an extension of this argument, anisotropic molecular and distributed LMO formulations use different **T** tensors (see eqs 37 and 38) and consequently yield different dispersion energies. Moreover, for E7 (LMO), the LMO dipole−quadrupole polarizability is also being transformed by the origin-shift formula (eq 27). In essence, the different definitions of the electrostatic **T** tensors and the origin shifting transformation are the causes of the discrepancy between the dispersion energies calculated with molecular and LMO formulations. Fundamentally, the two formulations express the interaction operator as two different expansions. The total dispersion energies calculated by the two expansions theoretically converge to the same value, just as the oscillator strengths based on the dipole length and the dipole velocity converge to the exact result in the limit of a full configuration interaction wave function. Conceptually the distributed formulation is expected to converge faster by the following argument. A molecular dipole can be regarded as two separated point charges, and a molecular quadrupole can be considered as arising from the separation of two dipoles. In other words, the distributed multipoles of lower rank may resemble molecular multipoles of higher rank.[44] Consequently, E6 (LMO) captures higher order dispersion terms such as E7 (molecular) and even higher order contributions. So, agreement between the two formulations will be achieved for the total dispersion energy when the molecular and distributed multipole expansions are carried out to complete order, although there is no one-to-one correspondence between the individual terms of the different expansions.

Figure 4 plots the E7 (LMO) values of two dimer systems, $(H_2O)_2$ and $(CH_4)_2$, at various intermolecular distances, from

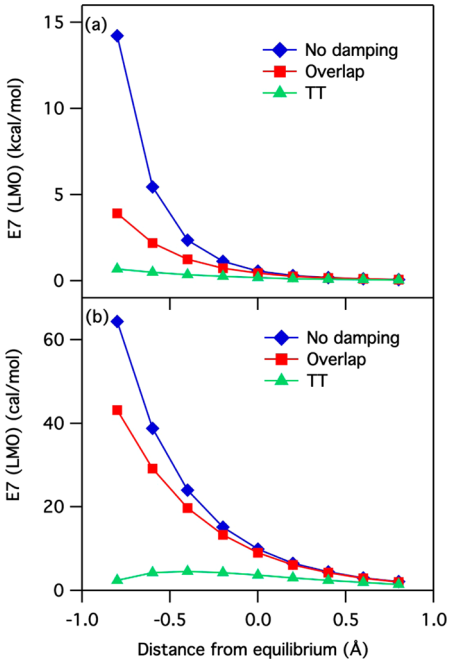

Figure 4. (a) Water (b) methane dimers: E7 (LMO) calculated at various intermolecular distances ranging from −0.8 to +0.8 Å away from the equilibrium distance. The effect of two types of damping function are also shown in the figure: the red squares represent the damped E7 (LMO) by an overlap-based damping function, and the green triangles represent the damped E7 (LMO) by the Tang−Toennies damping function.

−0.8 to 0.8 Å with respect to the equilibrium distance. Both undamped values and damped E7 (LMO) using the two different damping functions are plotted. As mentioned in Section II, the purpose of the damping function is to ensure the correct asymptotic behavior as R approaches zero. From Figure 4, the Tang−Toennies function appears to overdamp E7 (LMO), i.e., Tang−Toennies damped E7 (LMO) tends to be too weak at shorter intermolecular distances. Hence the overlap-based damping function is chosen to be the default damping option for EFP−EFP E7 (LMO) calculations.

Figure 5 compares the E6 (LMO) + E7 (LMO) dispersion energies for $(H_2O)_2$ and $(CH_4)_2$, with or without damping, to

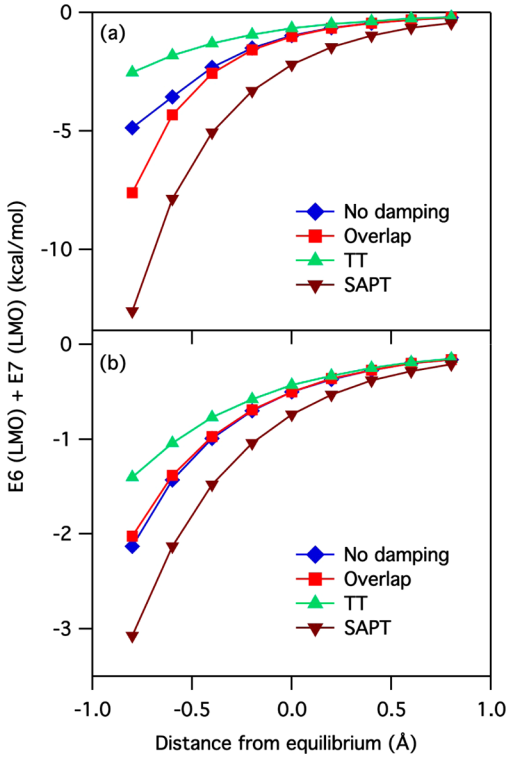

Figure 5. (a) Water (b) methane dimers: E6 (LMO) + E7 (LMO) dispersion energy calculated at various intermolecular distances ranging from −0.8 to 0.8 Å away from the equilibrium distance. The effect of the two types of damping function are also shown in the figure: the red squares represent the damped dispersion energy by an overlap-based damping function, and the green triangles represent the damped dispersion by the Tang−Toennies damping function. The SAPT numbers are shown as brown triangles.

the SAPT values. Overall, the overlap-damped dispersion curve resembles the SAPT curve better. At short intermolecular distances, the overlap-damped $(H_2O)_2$ dispersion energy appears to be more negative than the nondamped value although it is closer to the SAPT value. This is because the nondamped E7 (LMO) is positive and much larger than the overlap-damped E7 (LMO), which makes the sum of E6 and E7 less negative. The Tang−Toennies damping function shows the same overdamping problem noted above.

V. CONCLUSION AND FUTURE WORK

A general expression for the R^{-7} contribution to the dispersion energy between two molecular systems in the EFP framework has been derived and implemented in the GAMESS software package. The R^{-7} dispersion interaction can be computed using

either molecular (E7 (molecular)) or LMO (E7 (LMO)) dynamic dipole−quadrupole polarizability tensors over the imaginary frequency range. The molecular dynamic dipole−quadrupole polarizability is computed from the dipole response and the quadrupole moments. For E7 (LMO), the proper LMO dynamic dipole−quadrupole polarizabilities are obtained after an origin shift transformation from the center of mass to the centroids of the LMOs. Two types of damping functions, overlap-based and Tang−Toennies damping functions, have been implemented for the calculation of E7 (LMO). Both E7 (molecular) and E7 (LMO) magnitudes can change substantially, and their signs can also change as the relative orientations of the molecules change. In other words, E7 is highly orientation dependent. For systems with constrained configurations, e.g., molecular solids or crystal structures or reactions occurring on a surface, E7 could be a significant contribution to the total dispersion interaction. E7 is probably is not critical for room-temperature gas phase or liquid phase structures, where molecules are free to rotate and the E7 interactions are averaged out. The difference between the dispersion energies calculated with molecular and LMO polarizabilities is a manifestation of different expansions of the interaction operator truncated at a finite order. The comparison between SAPT with E6 + E7 values suggests that the dispersion series is not converged at E7 and at least R^{-8} dispersion term should be added. The distributed formulation is expected to converge faster. Although this work has been presented in the context of the effective fragment potential method, the conclusions that are drawn here are very likely applicable to fully quantum calculations as well.

In order to perform geometry optimizations and molecular dynamics simulations, gradients of the R^{-7} dispersion energy will be the focus of future studies.

APPENDIX

Since the dipole−quadrupole polarizability is origin dependent, the question to ask naturally is, is E7 also origin dependent? Suppose the shift of the expansion centers is $r^{A'}$ and $r^{B'}$ for molecule A and B, respectively. Accordingly, the dipole−quadrupole polarizabilities of A and B become

$$A^{A'}_{\alpha,\gamma\sigma} = A^{A}_{\alpha,\gamma\sigma} - \left(\frac{3}{2} r_{\gamma}^{A'} \alpha^{A}_{\sigma\alpha} + \frac{3}{2} r_{\sigma}^{A'} \alpha^{A}_{\alpha\gamma} - r_{\mu}^{A'} \alpha^{A}_{\mu\alpha} \delta_{\gamma\sigma}\right) \tag{A1}$$

$$A^{B'}_{\beta,\sigma\kappa} = A^{B}_{\beta,\sigma\kappa} - \left(\frac{3}{2} r_{\sigma}^{B'} \alpha^{B}_{\kappa\beta} + \frac{3}{2} r_{\kappa}^{B'} \alpha^{B}_{\beta\sigma} - r_{\mu}^{B'} \alpha^{B}_{\mu\beta} \delta_{\sigma\kappa}\right) \tag{A2}$$

The superscripts A and B denote the original expansion centers for molecules A and B, respectively. And A' and B' denote the new expansion centers. The subscripts denote the Cartesian coordinates x, y, and z. δ is the Kronecker delta function. Note that due to the origin-shift, the $\mathbf{T}$ tensors are also altered. Therefore now the E7 expression becomes

$$\begin{aligned}
E7 &= -\frac{\hbar}{3\pi} \mathbf{T}^{A'B'}_{\alpha\beta} \mathbf{T}^{A'B'}_{\gamma\sigma\kappa} \int_0^\infty d\omega [\alpha^{A'}_{\alpha\gamma}(i\omega) A^{B'}_{\beta,\sigma\kappa}(i\omega) - \alpha^{B'}_{\beta\kappa}(i\omega) A^{A'}_{\alpha,\gamma\sigma}(i\omega)] \\
&= -\frac{\hbar}{3\pi} \mathbf{T}^{A'B'}_{\alpha\beta} \mathbf{T}^{A'B'}_{\gamma\sigma\kappa} \int_0^\infty d\omega \\
&\quad \left[\begin{array}{l}
\alpha^{A}_{\alpha\gamma}(i\omega)\left(A^{B}_{\beta,\sigma\kappa}(i\omega) - \left(\frac{3}{2} r_{\sigma}^{B'} \alpha^{B}_{\kappa\beta}(i\omega) + \frac{3}{2} r_{\kappa}^{B'} \alpha^{B}_{\beta\sigma}(i\omega) \right.\right. \\
\quad \left.\left. - r_{\mu}^{B'} \alpha^{B}_{\mu\beta}(i\omega)\delta_{\sigma\kappa}\right)\right) \\
-\alpha^{B}_{\beta\kappa}(i\omega)\left(A^{A}_{\alpha,\gamma\sigma}(i\omega) - \left(\frac{3}{2} r_{\gamma}^{A'} \alpha^{A}_{\sigma\alpha}(i\omega) + \frac{3}{2} r_{\sigma}^{A'} \alpha^{A}_{\alpha\gamma}(i\omega) \right.\right. \\
\quad \left.\left. - r_{\mu}^{A'} \alpha^{A}_{\mu\alpha}(i\omega)\delta_{\gamma\sigma}\right)\right)
\end{array}\right]
\end{aligned} \tag{A3}$$

From eq A3, E7 calculated from these new polarizabilities, in general, do not necessarily equal to the E7 calculated previously.

However, if $r^{A'} = r^{B'} = r'$, i.e., uniform translation of the origins, the $\mathbf{T}$ tensors are unchanged because the intermolecular distance R that defines the $\mathbf{T}$ tensors remains the same. Now eq A3 becomes

$$\begin{aligned}
E7 &= -\frac{\hbar}{3\pi} T^{AB}_{\alpha\beta} T^{AB}_{\gamma\sigma\kappa} \int_0^\infty d\omega \left[\alpha^{A}_{\alpha\gamma}(i\omega)\left(A^{B}_{\beta,\sigma\kappa}(i\omega) \right.\right. \\
&\quad \left. - \left(\frac{3}{2} r'_{\sigma} \alpha^{B}_{\kappa\beta}(i\omega) + \frac{3}{2} r'_{\kappa} \alpha^{B}_{\beta\sigma}(i\omega) - r'_{\mu} \alpha^{B}_{\mu\beta}(i\omega)\delta_{\sigma\kappa}\right)\right) \\
&\quad - \alpha^{B}_{\beta\kappa}(i\omega)\left(A^{A}_{\alpha,\gamma\sigma}(i\omega) - \left(\frac{3}{2} r'_{\gamma} \alpha^{A}_{\sigma\alpha}(i\omega) + \frac{3}{2} r'_{\sigma} \alpha^{A}_{\alpha\gamma}(i\omega) \right.\right. \\
&\quad \left.\left. \left. - r'_{\mu} \alpha^{A}_{\mu\alpha}(i\omega)\delta_{\gamma\sigma}\right)\right)\right]
\end{aligned} \tag{A4}$$

The change in E7 is

$$\begin{aligned}
E7 &= -\frac{\hbar}{3\pi} \mathbf{T}^{AB}_{\alpha\beta} \mathbf{T}^{AB}_{\gamma\sigma\kappa} \int_0^\infty d\omega \left[- \alpha^{A}_{\alpha\gamma}(i\omega)\left(\frac{3}{2} r'_{\sigma} \alpha^{B}_{\kappa\beta}(i\omega) + \frac{3}{2} r'_{\kappa} \alpha^{B}_{\beta\sigma}(i\omega) \right.\right. \\
&\quad \left. - r'_{\mu} \alpha^{B}_{\mu\beta}(i\omega)\delta_{\sigma\kappa}\right) + \alpha^{B}_{\beta\kappa}(i\omega)\left(\frac{3}{2} r'_{\gamma} \alpha^{A}_{\sigma\alpha}(i\omega) + \frac{3}{2} r'_{\sigma} \alpha^{A}_{\alpha\gamma}(i\omega) \right. \\
&\quad \left.\left. - r'_{\mu} \alpha^{A}_{\mu\alpha}(i\omega)\delta_{\gamma\sigma}\right)\right] \\
&= -\frac{\hbar}{3\pi} \int_0^\infty d\omega \left[- \frac{3}{2} \mathbf{T}^{AB}_{\alpha\beta} \mathbf{T}^{AB}_{\gamma\sigma\kappa} r'_{\sigma} \alpha^{A}_{\alpha\gamma}(i\omega) \alpha^{B}_{\kappa\beta}(i\omega) \right. \\
&\quad - \frac{3}{2} \mathbf{T}^{AB}_{\alpha\beta} \mathbf{T}^{AB}_{\gamma\sigma\kappa} r'_{\kappa} \alpha^{A}_{\alpha\gamma}(i\omega) \alpha^{B}_{\beta\sigma}(i\omega) + \mathbf{T}^{AB}_{\alpha\beta} \mathbf{T}^{AB}_{\gamma\sigma\kappa} \alpha^{A}_{\alpha\gamma}(i\omega) r'_{\mu} \alpha^{B}_{\mu\beta}(i\omega)\delta_{\sigma\kappa} \\
&\quad + \frac{3}{2} \mathbf{T}^{AB}_{\alpha\beta} \mathbf{T}^{AB}_{\gamma\sigma\kappa} r'_{\gamma} \alpha^{B}_{\beta\kappa}(i\omega) \alpha^{A}_{\sigma\alpha}(i\omega) + \frac{3}{2} \mathbf{T}^{AB}_{\alpha\beta} \mathbf{T}^{AB}_{\gamma\sigma\kappa} r'_{\sigma} \alpha^{B}_{\beta\kappa}(i\omega) \alpha^{A}_{\alpha\gamma}(i\omega) \\
&\quad \left. - \mathbf{T}^{AB}_{\alpha\beta} \mathbf{T}^{AB}_{\gamma\sigma\kappa} \alpha^{B}_{\beta\kappa}(i\omega) r'_{\mu} \alpha^{A}_{\mu\alpha}(i\omega)\delta_{\gamma\sigma}\right]
\end{aligned} \tag{A5}$$

Since the dipole−dipole polarizability is symmetric with respect to interchange of the two suffixes, the first and the second last terms in eq A5 cancel each other. By the definition of the $\mathbf{T}$ tensors, the $\mathbf{T}$ tensors with two or more suffixes are invariant with respect to interchange of suffixes. The second and fourth terms can be rewritten as

$$\begin{aligned}
&-\frac{3}{2} \mathbf{T}^{AB}_{\beta\alpha} \alpha^{A}_{\alpha\gamma}(i\omega) \mathbf{T}^{AB}_{\gamma\sigma\kappa} r'_{\kappa} \alpha^{B}_{\sigma\beta}(i\omega) \\
&+\frac{3}{2} \mathbf{T}^{AB}_{\beta\alpha} \alpha^{A}_{\alpha\sigma}(i\omega) \mathbf{T}^{AB}_{\sigma\kappa\gamma} r'_{\gamma} \alpha^{B}_{\kappa\beta}(i\omega)
\end{aligned} \tag{A6}$$

Recall that Einstein summation convention is used here: a repeated subscript implies summation over that subscript. Therefore one can see that the two terms in A6 are equal in magnitude and opposite in sign and hence cancel each other. The third term in eq A5 is

dx.doi.org/10.1021/ct500017n | J. Chem. Theory Comput. 2014, 10, 1576−1587

$$\mathbf{T}^{AB}_{\alpha\beta}\mathbf{T}^{AB}_{\gamma\sigma\kappa}\alpha^{A}_{\alpha\gamma}(i\omega)r'_{\mu}\alpha^{B}_{\mu\beta}(i\omega)\delta_{\sigma\kappa} = (\mathbf{T}^{AB}_{\gamma\sigma\kappa}\delta_{\sigma\kappa})\alpha^{A}_{\gamma\alpha}(i\omega)\mathbf{T}^{AB}_{\alpha\beta}\alpha^{B}_{\beta\mu}(i\omega)r'_{\mu} \quad \text{(A7)}$$

The term in the parentheses

$$\begin{aligned}\mathbf{T}^{AB}_{\gamma\sigma\kappa}\delta_{\sigma\kappa} &= \mathbf{T}^{AB}_{\gamma\sigma\sigma}\\ &= \frac{15R_\gamma R_\sigma R_\sigma - 3R^2(R_\gamma\delta_{\sigma\sigma} + R_\sigma\delta_{\gamma\sigma} + R_\sigma\delta_{\gamma\sigma})}{R^7}\\ &= \frac{15R_\gamma R^2 - 3R^2(3R_\gamma + 2R_\sigma\delta_{\gamma\sigma})}{R^7}\\ &= \frac{15R_\gamma R^2 - 3R^2(3R_\gamma + 2R_\gamma)}{R^7}\\ &= \frac{15R_\gamma R^2 - 15R^2R_\gamma}{R^7}\\ &= 0\end{aligned} \quad \text{(A8)}$$

Again, the Einstein summation convention is implied here. Hence the third term, and similarly the last term, in eq A5 are both zero. So, overall E7 is unchanged when the origin shifts are the same for both molecules.

■ ASSOCIATED CONTENT

Supporting Information

Table of E7 (benchmark) and E7 (molecular), in Hartree, computed for different combination of (θ_A, θ_B, φ), with θ ranging from 0 to π and φ from 0 to $7\pi/4$ radians. This material is available free of charge via the Internet at http://pubs.acs.org.

■ AUTHOR INFORMATION

Corresponding Author

*E-mail: mark@si.msg.chem.iastate.edu

Notes

The authors declare no competing financial interest.

■ ACKNOWLEDGMENTS

This material is based upon work supported by the Air Force Office of Scientific Research under AFOSR Award No. FA9550-11-1-0099. The authors are grateful for very helpful discussions with Mr. Stephen Berg, Dr. Roger D. Amos, Professor Lyudmila Slipchenko, and Professor Piotr Piecuch.

■ REFERENCES

(1) Pruitt, S. R.; Leang, S. S.; Xu, P.; Fedorov, D. G.; Gordon, M. S. Hexamers and Witchamers: Which Hex Do You Choose? *Comput. Theor. Chem.* **2013**, *1021*, 70−83.

(2) Burley, S. K.; Petsko, G. A. Aromatic-Aromatic Interaction: A Mechanism of Protein Structure Stabilization. *Sci. (Washington, DC, U.S.)* **1985**, *229*, 23−28.

(3) Saenger, W. *Principles of Nucleic Acid Structure*; Springer-Verlag: New York, 1984; p 556.

(4) Lerman, L. S. Structural Considerations in the Interaction of Deoxyribonucleic Acid and Acridines. *Mol. Biol.* **1961**, *3*, 18−30.

(5) Brana, M. F.; Cacho, M.; Gradillas, A.; De B., P.-T.; Ramos, A. Intercalators as Anticancer Drugs. *Curr. Pharm. Des.* **2001**, *7*, 1745−1780.

(6) Eisenschitz, R.; London, F. The Relation between the van Der Weals Forces and the Homeopolar Valence Forces. *Z. Phys.* **1930**, *60*, 491−527.

(7) London, F. Theory and Systematics of Molecular Forces. *Z. Phys.* **1930**, *63*, 245−279.

(8) London, F. The General Theory of Molecular Forces. *Trans. Faraday Soc.* **1937**, *33*, 8−26.

(9) *The Theory of Intermolecular Forces*; Stone, A. J., Ed.; Oxford University Press: Oxford, 1996.

(10) Amos, R. D.; Handy, N. C.; Knowles, P. J.; Rice, J. E.; Stone, A. J. Ab Initio Prediction of Properties of Carbon Dioxide, Ammonia, and Carbon Dioxide...ammonia. *J. Phys. Chem.* **1985**, *89*, 2186−2192.

(11) Buckingham, A. D. Theory of Long-Range Dispersion Forces. *Discuss. Faraday Soc.* **1965**, *No. 40*, 232−238.

(12) Day, P. N.; Jensen, J. H.; Gordon, M. S.; Webb, S. P.; Stevens, W. J.; Krauss, M.; Garmer, D.; Basch, H.; Cohen, D. An Effective Fragment Method for Modeling Solvent Effects in Quantum Mechanical Calculations. *J. Chem. Phys.* **1996**, *105*, 1968−1986.

(13) Stone, A. J. Distributed Multipole Analysis, or How to Describe a Molecular Charge Distribution. *Chem. Phys. Lett.* **1981**, *83*, 233−239.

(14) Stone, A. J.; Alderton, M. Distributed Multipole Analysis Methods and Applications. *Mol. Phys.* **1985**, *56*, 1047−1064.

(15) Jensen, J. H.; Gordon, M. S. An Approximate Formula for the Intermolecular Pauli Repulsion between Closed Shell Molecules. *Mol. Phys.* **1996**, *89*, 1313−1325.

(16) Li, H.; Gordon, M. S.; Jensen, J. H. Charge Transfer Interaction in the Effective Fragment Potential Method. *J. Chem. Phys.* **2006**, *124*, 214108/1−214108/16.

(17) Xu, P.; Gordon, M. S. Charge Transfer Interaction Using Quasiatomic Minimal-Basis Orbitals in the Effective Fragment Potential Method. *J. Chem. Phys.* **2013**, *139*, 194104/1−194104/11.

(18) Adamovic, I.; Gordon, M. S. Dynamic Polarizability, Dispersion Coefficient C6 and Dispersion Energy in the Effective Fragment Potential Method. *Mol. Phys.* **2005**, *103*, 379−387.

(19) Smith, Q. A.; Ruedenberg, K.; Gordon, M. S.; Slipchenko, L. V. The Dispersion Interaction between Quantum Mechanics and Effective Fragment Potential Molecules. *J. Chem. Phys.* **2012**, *136*, 244107/1−244107/12.

(20) Casimir, H. B. G.; Polder, D. The Influence of Retardation on the London-van Der Waals Forces. *Phys. Rev.* **1948**, *73*, 360−372.

(21) Gross, E. K. U.; Ullrich, C. A.; Gossmann, U. J. Density Functional Theory of Time-Dependent Systems. *NATO ASI Ser., Ser. B* **1995**, *337*, 149−171.

(22) Stone, A. J. Distributed Polarizabilities. *Mol. Phys.* **1985**, *56*, 1065−1082.

(23) Stone, A. J.; Tong, C. S. Local and Nonlocal Dispersion Models. *Chem. Phys.* **1989**, *137*, 121−135.

(24) Williams, G. J.; Stone, A. J. Distributed Dispersion: A New Approach. *J. Chem. Phys.* **2003**, *119*, 4620−4628.

(25) Jensen, J. H.; Gordon, M. S. Ab Initio Localized Charge Distributions: Theory and a Detailed Analysis of the Water Dimer-Hydrogen Bond. *J. Phys. Chem.* **1995**, *99*, 8091−8107.

(26) England, W.; Gordon, M. S. Localized Charge Distributions. I. General Theory, Energy Partitioning, and the Internal Rotation Barrier in Ethane. *J. Am. Chem. Soc.* **1971**, *93*, 4649−4657.

(27) England, W.; Gordon, M. S. Localized Charge Distributions. II. Interpretation of the Barriers to Internal Rotation in Hydrogen Peroxide. *J. Am. Chem. Soc.* **1972**, *94*, 4818−4823.

(28) Gordon, M. S.; England, W. Localized Charge Distributions. III. Transferability and Trends of Carbon-Hydrogen Moments and Energies in Acyclic Hydrocarbons. *J. Am. Chem. Soc.* **1972**, *94*, 5168−5178.

(29) Gordon, M. S.; England, W. Localized Charge Distributions. Internal Rotation Barrier in Borazane. *Chem. Phys. Lett.* **1972**, *15*, 59−64.

(30) Gordon, M. S.; England, W. Localized Charge Distributions. V. Internal Rotation Barriers in Methylamine, Methyl Alcohol, Propene, and Acetaldehyde. *J. Am. Chem. Soc.* **1973**, *95*, 1753−1760.

(31) Gordon, M. S. Localized Charge Distributions. VI. Internal Rotation in Formaldoxime and Formic Acid. *J. Mol. Struct.* **1974**, *23*, 399−410.

(32) England, W.; Gordon, M. S.; Ruedenberg, K. Localized Charge Distributions. VII. Transferable Localized Molecular Orbitals for Acyclic Hydrocarbons. *Theor. Chim. Acta* **1975**, *37*, 177−216.

(33) Quinet, O.; Liegeois, V.; Champagne, B. TDHF Evaluation of the Dipole-Quadrupole Polarizability and Its Geometrical Derivatives. *J. Chem. Theory Comput.* **2005**, *1*, 444−452.
(34) Tang, K. T.; Toennies, J. P. An Improved Simple Model for the van Der Waals Potential Based on Universal Damping Functions for the Dispersion Coefficients. *J. Chem. Phys.* **1984**, *80*, 3726−3741.
(35) Slipchenko, L. V; Gordon, M. S. Damping Functions in the Effective Fragment Potential Method. *Mol. Phys.* **2009**, *107*, 999−1016.
(36) Schmidt, M. W.; Baldridge, K. K.; Boatz, J. A.; Elbert, S. T.; Gordon, M. S.; Jensen, J. H.; Koseki, S.; Matsunaga, N.; Nguyen, K. A.; et al. General Atomic and Molecular Electronic Structure System. *J. Comput. Chem.* **1993**, *14*, 1347−1363.
(37) Gordon, M. S.; Schmidt, M. W. Advances in Electronic Structure Theory: GAMESS a Decade Later. In *Theory and Applications of Computational Chemistry: The First Forty Years*; Elsevier B.V.: Amsterdam, The Netherlands, 2005; pp 1167−1189.
(38) Meyer, W. Dynamic Multipole Polarizabilities of Hydrogen and Helium and Long-Range Interaction Coefficients for Hydrogen-Hydrogen, Hydrogen-Helium and Helium-Helium. *Chem. Phys.* **1976**, *17*, 27−33.
(39) Bendazzoli, G. L.; Magnasco, V.; Figari, G.; Rui, M. Full-CI Calculation of Imaginary Frequency-Dependent Dipole Polarizabilities of Ground State LiH and the C6 Dispersion Coefficients of LiH-LiH. *Chem. Phys. Lett.* **2000**, *330*, 146−151.
(40) Luigi Gian, B.; Magnasco, V.; Figari, G.; Rui, M. Full-CI Calculation of Imaginary Frequency-Dependent Dipole-Quadrupole Polarizabilities of Ground State LiH and the C7 Dispersion Coefficients of LiH-LiH. *Chem. Phys. Lett.* **2002**, *363*, 540−543.
(41) Bendazzoli, G. L.; Monari, A.; Magnasco, V.; Figari, G.; Rui, M. An Enlarged Basis Full-CI Calculation of C7 Dispersion Coefficients for the LiH-LiH Homodimer. *Chem. Phys. Lett.* **2003**, *382*, 393−398.
(42) Luigi Gian, B.; Magnasco, V.; Figari, G.; Rui, M. Full-CI Calculation of Imaginary Frequency-Dependent Dipole-Quadrupole Polarizabilities of Ground State LiH and the C7 Dispersion Coefficients of LiH-LiH. [Erratum to Document Cited in CA137:358415]. *Chem. Phys. Lett.* **2003**, *381*, 526−527.
(43) Jeziorski, B.; Moszynski, R.; Szalewicz, K. Perturbation Theory Approach to Intermolecular Potential Energy Surfaces of van Der Waals Complexes. *Chem. Rev. (Washington, DC, U.S.)* **1994**, *94*, 1887−1930.
(44) Buckingham, A. D. Molecular Quadrupole Moments. *Q. Rev.* **1959**, *8*, 183−214.